Printed monopole antenna with tunable band-notched characteristic for use in mobile and ultra-wide band applications

International Journal of RF and Microwave Computer-Aided Engineering, vol. 25, no. 5, pp. 403-412, June 2015, Article first published online: 6 NOV 2014, Wiley Online Library, DOI: 10.1002/mmce.20874; Online ISSN: 1099-047X.

Printed Monopole Antenna with Tunable Band-Notched Characteristic for Use in Mobile and UWB Applications

I.T.E. Elfergani[1], A.S. Hussaini[1,5], R.A. Abd-Alhameed[3], C.H. See[3, 4], N. J. McEwan[3],S. Zhu[3], J. Rodriguez[1,2] and R.W. Clarke[3]

[1]Instituto de Telecomunicações, Aveiro, Portugal

[2]Universidade de Aveiro, Portugal

[3]Radio Frequency, Antennas, Propagation and Computational Electromagnetics Research Group, School of Electrical Engineering and Computer Sciences, University of Bradford, Bradford, BD7 1DP, UK

[4]Engineering, Sport and Science (ESS) Academic Group, University of Bolton, Bolton, BL3 5AB, UK

[5]Department of Electrical & Electronics Engineering Modibbo Adama University of Technology, Yola Nigeria

ABSTRACT

A tunable band-notch printed monopole antenna is presented, exhibiting a wide impedance bandwidth from 1.5 to 5.5 GHz with good impedance matching (VSWR $\leq$ 2) and a tunable rejected frequency band from 2.38 to 3.87 GHz. The band-notching is achieved by adding an inner chorded crescent element within a driven element of a similar shape. By varying the value of the varactor which is placed between the inner and outer arcs, the desired variable rejected can be obtained. Simulated and measured results show wide impedance bandwidth with a tunable band notch, stable radiation patterns, and consistent nearly constant gain. The antenna is suitable for mobile and portable applications.

Index Terms— Wideband antenna, Tunable notch, Varactor diode, Monopole antenna.

International Journal of RF and Microwave Computer-Aided Engineering, vol. 25, no. 5, pp. 403-412, June 2015, Article first published online: 6 NOV 2014, Wiley Online Library, DOI: 10.1002/mmce.20874; Online ISSN: 1099-047X.

I. INTRODUCTION

The printed wideband monopole antenna has been widely adopted in commercial and military applications. With attractive features such as low cost, small size and ease of fabrication, this antenna has received increasing attention with developments in communication technology. Many versions have been reported over the last decade [1-12], covering a wide range of frequency bands and diverse applications.

However, due to the coexistence of different wireless standards, radiation in some of these frequency bands may generate interference to (or from) the communication systems such as the Wireless local area networks (WLAN) of IEEE802.11b/g and IEEE802.11a standard (2.4–2.485 GHz) and Worldwide Interoperability for Microwave Access for IEEE802.16 bands (2.5–2.69 GHz, 3.3–3.7 GHz) bands. In an Ultra-wide band (UWB) system, owing to its low power emission characteristic, interference has become a serious problem and the UWB antenna requires a band-suppression feature. Popular methods of adding the frequency band-notch function are embedding slots [13-16], introducing different shapes of parasitic strip radiator [17], defected ground structure (DGS) [18], or employing slots and DGS methods simultaneously [19]. Table I shows the differences between these antennas in terms of operating frequency band, impedance bandwidth, antenna size, tunability, and tunable notched frequency range.

Table I shows clearly that these antennas [13-19] cannot simultaneously cover mobile and UWB applications. For example, the designs in [17-19] are only capable of operating in UWB applications while antenna geometries in [13-15] can cover the mobile bands of the

International Journal of RF and Microwave Computer-Aided Engineering, vol. 25, no. 5, pp. 403-412, June 2015, Article first published online: 6 NOV 2014, Wiley Online Library, DOI: 10.1002/mmce.20874; Online ISSN: 1099-047X.

universal mobile telecommunications system (UMTS) (1.92–2.17 GHz), IEEE 802.11 a/b/g (2.4–2.485 GHz, 5.15–5.35 GHz) and lower band UWB (3.1 – 4.8 GHz). In contrast to [13-19], this paper reports a printed tunable notch monopole antenna that achieves a size reduction and has the potential to simultaneously cover both mobile and UWB communication applications from 1.5 to 5.5 GHz except at the Wireless local area networks (WLAN) of IEEE802.11b/g and IEEE802.11a standard (2.4–2.485 GHz) and World Interoperability for Microwave Access (WIMAX) for IEEE802.16 bands (2.5–2.69 GHz, 3.3–3.7 GHz) bands.

Moreover, these antennas [13-19] have fixed rejected frequency bands which cannot be altered after fabrication. Recent studies considered adaptive frequency suppression methods using switched PIN diode [20, 21] and varactor diode [22-27] techniques. These allow easy rejection of variable interference using components internal to the antenna, thus minimizing size increase and losses.

By compromising between the bandwidth, antenna size and tunable frequency range of notched antennas, some tuning methods were proposed in [20–27] to enable multi-notch operation, as shown in Table I. In comparison with these, [20-27], the present antenna design has advantages of covering mobile and UWB application with a targeted band notch as compared to [22-24,26-27], and of operating in other existing wireless bands such as GPS/L1(1.565–1.585 GHz), Iridium satellite band (1.616–1.6265 GHz), personal communications service (PCS) band (1.85–1.99 GHz), digital cellular service (DCS) band (1.71–1.88 GHz) in contrast to [25]. Also, it accomplishes a size reduction compared with [20-27].

International Journal of RF and Microwave Computer-Aided Engineering, vol. 25, no. 5, pp. 403-412, June 2015, Article first published online: 6 NOV 2014, Wiley Online Library, DOI: 10.1002/mmce.20874; Online ISSN: 1099-047X.

In summary, it is found that most of the fixed notch antennas cannot fully cover many existing mobile standards [13-15] or the UWB spectrum [17-19]. One can also note that most of the tunable notch antennas will only cover UWB systems [22-24, 26-27], except for the work in [20-25] in which they also covered some existing mobile spectrum. To address this limitation, a printed monopole antenna with tunable notch is investigated in this present work. This is a modified version of the antenna presented in [11, 16], and our main purpose here is to realize the idea of electronically tuning the band notch already created. This has been done by accommodating a varactor diode at the appropriate position between the two chorded crescent shapes. By varying its capacitance from 0.25 to 10.5pF, the notch band can be swept downwards over a wide range from 3.5 GHz to 2.4 GHz to cover the Wireless local area networks (WLAN) of the IEEE802.11b/g and IEEE802.11a standards (2.4–2.485 GHz) and World Interoperability for Microwave Access (WIMAX) in IEEE802.16 bands (2.5–2.69 GHz, 3.3–3.7 GHz).

II. ANTENNA DESIGN CONCEPTS AND STRUCTURE

The antenna geometry is shown in Fig. 1a. It consists of a driven two chorded crescent-shaped radiator, which is similar to our previous work [11,16]. Prototypes have been printed on an FR4 material of thickness 0.8mm, relative permittivity $\varepsilon_r = 4.4$ and loss tangent 0.017, with no ground plane directly underneath the radiator. The latter is fed by a 17.95×1 mm microstrip line, printed on the portion of the substrate that lies over the ground plane. The microstrip line has an upper section (6.75 mm) and a lower section (11.25 mm). The lower section has a characteristic impedance of 64 Ω and is required for matching to the 50 Ω input port at the lower edge of the ground plane. It should be noted that the defected area size 24.75 mm × 26.25 mm located on the top of the ground plane is introduced to reduce the Q of the

International Journal of RF and Microwave Computer-Aided Engineering, vol. 25, no. 5, pp. 403-412, June 2015, Article first published online: 6 NOV 2014, Wiley Online Library, DOI: 10.1002/mmce.20874; Online ISSN: 1099-047X.

radiator and so raise the impedance bandwidth at the input port of the antenna. The antenna was modelled using the both HFSS [28] and SEMCAD software packages [29].

The simulated VSWRs of the crescent and chorded crescent-shaped antennas, with complete and defected ground plane, are shown in Fig. 1b. As would be expected, removing a section of ground plane under the radiator reduces stored energy and greatly improves the impedance matching bandwidth. The total dimension of the proposed antenna is 57 mm × 37.5 mm which is acceptable for application in a mobile device. The wider impedance bandwidth characteristic of the proposed antenna can be realized by adding a chordal strip to the outer crescent shape, as in [11]. This antenna is a modified version of that in [11,16], but has a larger bandwidth than reported in [11], and offers a tunable notched band characteristic in contrast to [16]. The notched band was achieved by adding an inner chorded crescent shape to a chorded crescent shape similar to that presented in [16].

The design procedure of this antenna is elaborated here to offer some physical insight into its operation and the rationale for its geometry. The design process starts from modifying the geometry of the chorded crescent-shaped antenna in [16] to provide wide tunable rejected bands to cover coexisting WLAN (2.4 – 2.485 GHz) and WiMAX (3.3 – 3.7 GHz). Fig. 2 plots and compares the VSWR of the proposed antenna without a varactor and the antenna in [16]. It was interesting to observe that a 4.25 GHz centered notched band can be achieved by adding an inner chorded crescent shape with the outer chorded crescent shape presented in [16], but without a tapered sickle-shaped slot in the outer radiator. This is because the parasitic inner chorded crescent shape has a length of approximately 36.5 mm which is equivalent to a half-wavelength at 4.25 GHz. As a result, this structure acts as a resonator to

International Journal of RF and Microwave Computer-Aided Engineering, vol. 25, no. 5, pp. 403-412, June 2015, Article first published online: 6 NOV 2014, Wiley Online Library, DOI: 10.1002/mmce.20874; Online ISSN: 1099-047X.

suppress a band of frequencies around 4.25 GHz. However, this rejection frequency does not meet the design objective and a varactor is therefore required to down-shift it. With the proposed structure, that helps in accommodating the varactor at a fixed location between the two chorded crescent shapes for tuning the rejection band. Moreover this also enables the outer and inner shapes to be completely separated and not short circuit the dc potential difference across the varactor when it is implemented in practice.

To further investigate the physical behavior of the antenna, the input impedance of the proposed antennas (without varactor, with 0.5 pF or 10.5 pF varactor) and the reference antenna [16] are compared and analyzed in Fig. 3. At the lowest usable frequency band from 1.5 to 3 GHz, both the reference and proposed antennas show a linear increment of resistance (from 28 to 55 ohm) and reactance varying from 4 to -25 ohm. Thus antennas exhibit a better impedance matching at this frequency band. It is seen that two adjacent resonant frequencies, i.e. 1.7 and 2.75 GHz, can be found at the points where the reactance is zero and the resistance is almost 50 ohm.

At the higher usable operating frequency band from 3 to 5.5 GHz, the reference antenna show a changing resistance value between 40 to 50 ohm and reactance value between -8 to 30 ohm. This response satisfies the good impedance matching condition to a 50 ohm load. The impedance response of the proposed antenna without varactor shows a linear drop of the resistance (from 50 to 10 ohm) from 3 to 4.25 GHz. After that, the resistance curve drastically increases from 10 to 100 ohm and then drops sharply to 33 ohm. This indicates a typical series-resonance and a parallel-resonant behavior occur at around 4.25 GHz and 4.75 GHz. When the proposed antenna is loaded with 0.5 pF varactor, it is clearly observed that at the band-notched frequency 3.5 GHz, the reactance of this antenna becomes zero and the

International Journal of RF and Microwave Computer-Aided Engineering, vol. 25, no. 5, pp. 403-412, June 2015, Article first published online: 6 NOV 2014, Wiley Online Library, DOI: 10.1002/mmce.20874; Online ISSN: 1099-047X.

resistance value drops to its lowest value (4 ohm). Noticeably, this resistance value is almost constant (less than 10 ohm) across the unwanted frequency band (3.3 – 3. 7 GHz). Likewise, when the 10.pF varactor is used, the band-notched frequency shifts to 2.4 GHz with zero reactance and resistance reduces to its lowest value (5 ohm). This response exhibits a typical band-suppression characteristic.

By optimizing and studying the current surface of the proposed antenna, the position of the varactor is so selected as to achieve maximum frequency tuning while least perturbing the antenna matching. Its variable capacitance modifies the effective length of the inner chorded shape.

III. RESULTS AND DISCUSSION

Fig. 2 shows the simulated VSWR for the proposed antenna with the inner chorded crescent shape and both inner and outer chorded crescent shapes. As can be seen in Fig. 2, by adding a strip to the outer crescent shape the proposed antenna resonates from 1.5 to 5.5 GHz, achieving a wider frequency range compared to the authors' previous work [11]. It should be noted that the outer radiator is constructed from sections of two circles, each having a different radius and center, thus enabling the resultant patch, taken with the effect of the coupling to the defected ground plane, to radiate over two different frequency bands. The larger radius controls the fundamental frequency, whilst the shorter radius may be tuned to obtain the desired upper frequency. It is clearly seen that the two adjacent resonant frequencies in the range VSWR $\leq$ 2, are 1.5 GHz and 5GHz, and it is worth noting that the

International Journal of RF and Microwave Computer-Aided Engineering, vol. 25, no. 5, pp. 403-412, June 2015, Article first published online: 6 NOV 2014, Wiley Online Library, DOI: 10.1002/mmce.20874; Online ISSN: 1099-047X.

antenna's impedance bandwidth is 3.5 GHz. This provides adequate coverage for GPS, DCS, PCS, UMTS, WLAN and WiMAX bands.

A. Varactor and the DC Bias Circuits of Proposed Antenna

The practicalities of frequency tuning of the proposed antenna, using varactor loading with a suitable DC bias circuit, were further explored. The packaged BBY52-02W varactor diode has capacitance tunable from 0.25 to 10.5 pF over the 0 to 15 V reverse bias voltage range. DC components for controlling the varactor are fitted on the back side of the PCB board, as depicted in Fig.4. The DC voltage is isolated from the RF signal using a radio-frequency choke of 100 nH with high-Q (>40), a tolerance of ± 5%. The chip inductors feature a monolithic body made of low loss ceramic wound with wire to achieve optimal high frequency performance. Two 100 pF chip capacitors provide DC blocking in the microstrip feed line and DC isolation of the short-circuited back strip. The capacitors used in this measurement are miniature multi-layer ceramic capacitors with high Q (>40) and ultra-low equivalent series resistance.

For better understanding the cable effect on the antenna performance, an antenna model with a DC cable is simulated as shown in Fig. 5. This study was performed by gradually increasing the total length of the wire from 30mm to 70mm and keeping the width at 0.5mm. As can be clearly illustrated, the variation VSWR along with targeted notch at 3.5GHz over the aforementioned lengths are more or less same when the a 0.5pF varactor is considered.

International Journal of RF and Microwave Computer-Aided Engineering, vol. 25, no. 5, pp. 403-412, June 2015, Article first published online: 6 NOV 2014, Wiley Online Library, DOI: 10.1002/mmce.20874; Online ISSN: 1099-047X.

The loaded proposed antenna prototype PCB along with varactor diode and passive components is shown in Figs. 4b and 4c. It can be seen from the measurement results that by varying the varactor DC bias from 5 V and 11V the band-notch center frequency would be tuned to reject the band of WLAN (2.4–2.485 GHz) and WIMAX (3.3-3.7 GHz) as shown in Fig. 6. A satisfactory continuously tunable notch occurs at all intermediate bias voltages.

B. The Current Surface of Varactor Proposed Antenna

For better understanding the effectiveness of the varactor, the current surface of the antenna with and without the varactor was investigated in Fig. 7 at the center-rejected frequency of 2.4 GHz and 3.5 GHz. As shown in Fig. 7(a), the major currents for unloaded antenna at 2.4 and 3.5GHz appear around the feed point as the notched band was not created. However, when a 0.5 pF is inserted in the proposed antenna to introduce the 3.5 GHz notched band, as can be seen in Fig. 7 (b), the current is heavily trapped in the antenna's radiator and it acts as a resonator. Likewise, when a 10.5 pF is added for generating the 2.4 GHz filtered band as shown in Fig. 7(c), again the strong current intensity presents on the antenna radiator that is similar to the case of 3.5 GHz.

C. Radiation Patterns, Power Gain and Efficiency of the Antenna

Radiation patterns of the prototype antenna were measured in a far-field anechoic chamber using an elevation-over-azimuth positioner, with the elevation axis coincident with the polar axis ($\theta = 0^0$) of the antenna's coordinate system. It should be noted that the coordinate system is defined in Fig.1, while θ is measured from positive Z-axis toward the XY plane and ϕ is calculated positive counter-clockwise from the X-axis in the XY plane.

International Journal of RF and Microwave Computer-Aided Engineering, vol. 25, no. 5, pp. 403-412, June 2015, Article first published online: 6 NOV 2014, Wiley Online Library, DOI: 10.1002/mmce.20874; Online ISSN: 1099-047X.

The azimuth drive thus generated cuts at constant ϕ. The reference fixed antenna was a broadband horn (EMCO type 3115) positioned at 4 m from the antenna under test. The elevation positioner was rotated over $\phi \in [-180^0, 180^0]$ in 5^0 increments. Two pattern cuts (i.e. the *xz* and *yz* planes) were taken at three selected operating frequencies, covering approximately most designated bandwidth. The prototype's radiation patterns at 1.6, 3.2 and 5.0 GHz when the varactor diode was excited by 5V and 11V were measured, and the corresponding results cross validated with the simulation data as shown in Fig. 8. The results show that the radiation patterns are nearly omnidirectional with distorted short-dipole characteristics especially the simulated ones. It is noticeable that some discrepancy between the simulated and measured patterns due to subtle differences between the simulated and physical feeding arrangements. Moreover, because the issue of polarisation purity is not critical for antennas used in portable devices, the high co- and cross- polarisation ratio of this antenna is acceptable. In addition, the radiation patterns with the varactor excited at 11V were quite consistent with those at 5V, and thus they are not presented here.

Fig. 9 shows the measured gain and the radiation efficiency of the monopole antenna in the case of unloaded and loaded design. It is noted that the presence of the varactor only shifts the notches and the gain does not change substantially. The unloaded antenna has a gain of 2.8 dBi at the notch band center frequency of 3.5GHz and 1.9 dBi at 2.48GHz .The peak antenna gain at 5V dc excitation is reduced to -9 dBi and to -7.5dBi at 11V. This indicates that there is approximately 11.8 dB and 9.4dB of gain suppression for the DC of 5V and 11V corresponding to equivalent fixed lumped element capacitors of 0.5pf and 10 pf respectively. The radiation efficiency curves of the analyzed models correspond well with the changes of the gain curves. The radiation efficiency been determined by using Wheeler Cap method

International Journal of RF and Microwave Computer-Aided Engineering, vol. 25, no. 5, pp. 403-412, June 2015, Article first published online: 6 NOV 2014, Wiley Online Library, DOI: 10.1002/mmce.20874; Online ISSN: 1099-047X.

[30], which is a well - accepted experimental method of finding the practical efficiency [31]. It can be observed in Fig. 9 that the efficiencies are all around 80% over the wide band from 1.5 to 5.5GHz, except in the notch bands at 4.25GHz of unloaded antenna and 3.5GHz/2.4GHz when the antenna loaded with 0.5pF and 10.5pF respectively where the efficiencies dropped to below 22%.

IV. CONCLUSION

A crescent-shaped antenna geometry with a tunable notch has been designed and presented. The proposed antenna occupies an envelope dimension of 57 × 37.5 × 0.8 mm^3 while covering the required wide band with a sufficiently tunable rejection frequency band ranging from WLAN (2.4–2.485 GHz) to WIMAX (3.3-3.7 GHz). The notch center frequency shift was quite stable and consistent over the selected spectrum without a serious change in notch bandwidth. The measured and simulated results using the lumped fixed capacitors and varactor diode are in good agreement. The antenna can satisfy typical requirements of bandwidth and interference reduction arising from current trends in wireless communications.

ACKNOWLEDGMENT

This work is carried out under the BENEFIC project (CA505), a project labelled within the framework of CATRENE, the EUREKA cluster for Application and Technology Research in Europe on NanoElectronics, co-financed by the European Funds for Regional Development (FEDER) by COMPETE – Programa Operacional do Centro (PO Centro) of QREN [Project

International Journal of RF and Microwave Computer-Aided Engineering, vol. 25, no. 5, pp. 403-412, June 2015, Article first published online: 6 NOV 2014, Wiley Online Library, DOI: 10.1002/mmce.20874; Online ISSN: 1099-047X.

number 38887 – BENEFIC. Also, this work has been performed in the framework of ARTEMOS project under work programme ENIAC JU 2010 and FCT (Fundação para a Ciência e Tecnologia). The authors would like to thank Datong PLC (Leeds LS18 4EG, West Yorkshire, U.K.), for their partial financial support of the Knowledge Transfer Partnership (KTP No: 008734).

Authors Affiliations:

I.T.E.Elfergani, A.S. Hussaini and J. Rodriguez with Instituto de Telecomunicações, Aveiro, Portugal
E-mail: i.t.e.elfergani@av.it.pt, ash@av.it.pt, jonathan@av.it.pt

R. A. Alhameed, C.H. See , N. J. McEwan and R.W. Clarke are with School of Engineering, Design and Technology, Bradford University Bradford, BD7 1DP, UK;
Email:
r.a.a.abd@bradford.ac.uk, c.h.see2@bradford.ac.uk, n.j.mcewan@bradford.ac.uk, Sharon.Zhu@7techgroup.com

REFERENCES

[1] F. Yang, X. Zhang, X.Ye, and Y. Rahmat-Samii, "Wide-Band E Shaped Patch Antennas for Wireless Communications," *IEEE Trans.Antennas Propagat.*, vol.49, no.7, pp. 1094-1099, July 2001

[2] Y.C. Lee and J.S. Sun" Compact Printed Slot Antennas for Wireless Dual- and Multi-Band Operations," *Progress In Electromagnetics Research*, vol. 88, pp. 289–305, 2008

[3] R. Zhu, X. Wang, and G. Yang, "A Wideband Monopole Antenna Using Parasitic Elements," *Applied Mechanics and materials, Trans. Tech. Publications*, Switzerland, Vol. 52–54, pp. 1515-1519, 2011.

[4] C.F. Tseng, C.L. Huang, C.H. Hsu, "Microstrip-Fed Monopole Antenna with a Shorted Parasitic Element for Wideband Application," *Progress In Electromagnetics Research Letters*, Vol. 7, pp. 115–125, 2009.

[5] H-D. Chen, "Broadband CPW-Fed Square Slot Antennas with a Widened Tuning Stub," *IEEE Trans. Antennas Propagat.,* vol. 51, no.8, pp. 1982-1986, Aug. 2003.

International Journal of RF and Microwave Computer-Aided Engineering, vol. 25, no. 5, pp. 403-412, June 2015, Article first published online: 6 NOV 2014, Wiley Online Library, DOI: 10.1002/mmce.20874; Online ISSN: 1099-047X.

[6] A.T.Mobashsher, B.Bais, N.Misran and M.T.Islam "Compact Wideband Microstrip Antenna for Universal 5GHz WLAN Applications" *Australian Journal of Basic and Applied Sciences*, Vol.4, No.8, pp.3411-3417, 2010.

[7] Y.W. Jang, "Broadband cross-shaped microstrip-fed slot antenna," *Electron. Lett.*, vol.25, pp. 2056-2057, 2000

[8] S. T. Fan, Y. Z. Yin, W. Hu, K. Song, and B. Li, "Novel CPW-Fed Printed Monopole Antenna with an N-Shaped Slot for Dual-Band Operations" *Microwave and Optical Technology Letters*, Vol. 54, No. 1 pp.240-242, Jan. 2012.

[9] M. Abbaspour and H. R. Hassani, "WideBand Star-Shaped Microstrip Patch Antenna," *Progress In Electromagnetics Research Letters*, Vol. 1, 61–68, 2008.

[10] M. Koohestani, M. Khaghani and H. Asadi, "A Compact Wideband Antenna with CPW-fed Monopole for WLAN/WiMAX Operation," *Journal of Telecommunications*, Vol. 10, No. 2, pp. 10-13, Sept. 2011.

[11] C.H. See, R. A. Abd-Alhameed, D. Zhou, T. H. Lee, and P.S. Excell, "A Crescent-Shaped Multiband Planar Monopole Antenna for Mobile Wireless Applications," *IEEE Antennas Wireless Propag. Lett.*, vol. 9, pp. 152–155, 2010.

[12] A.E. Alkurbo, S.H.Pramono, D.R.Santoso, "Design and Construct of Broadband Printed Rectangular Monopole Antenna," *IOSR Journal of Electronics and Communication,* Vol. 2, no. 4, pp. 20-24, 2012

[13] W.S.Chen, P.Y. Chang, B.Y. Lee, H.T.Chen and J-S.Kuo, "A Compact Microstrip-Fed Slot Antenna with a Dual-Band Notched function for WiMAX Operation", *Antennas and Propagation Society International Symposium (APSURSI)*, pp. 1-4, 2010.

[14] W.S.Lee, D.Z.Kim, K.J.Kim, and J.W.Yu, "Wideband Planar Monopole Antennas with Dual Band-Notched Characteristics," *IEEE Transactions On Microwave Theory And Techniques*, Vol.54, No. 6, pp.2800-2806. Jun. 2006.

[15] W.S.Lee, D.Z.Kim, and J.W. Yu, "Wideband Crossed Planar Monopole Antenna With The Band-Notched Characteristic," *Microwave and Optical Technology Letters*, Vol. 48, No. 3, pp.543-545. March 2006.

[16] C.H. See, R. A. Abd-Alhameed, F. Elmegri, D. Zhou J. M.Noras, N.J. McEwan, S.M.R. Jones and P. S. Excell, "Planar Monopole Antennas for New Generation Mobile and Lower Band Ultra-wide Band Applications," *IET Microw. Antennas Propag*, vol.6, no.11, pp.1207-1214, 2012.

[17] K.S .Ryu , A.A Kishk, "UWB antenna with single or dual band-notches for lower WLAN band and upper WLAN band", *IEEE Trans. Antennas Propag*., vol.57, no.12, pp. 3942–3950, 2009

[18] Y.B. Yang, F.S. Zhang, F. Zhang, L. Zhang, and Y-C. Jiao, "Design of novel wideband monopole antenna with a tunable notched-band for 2.4 GHz WLAN and UWB applications," *Progress In Electromagnetics Research Letters*, Vol. 13, pp. 93-102, 2010.

[19] P. Moeikham, C. Mahatthanajatuphat, and P. Akkaraekthalin" A Compact Ultra Wide-Band Monopole Antenna with 5.5GHz Notched Band," *Progress In Electromagnetics Research C*, Vol. 26, pp. 13-27, 2012.

[20] J. P.Carrier, P. P.Carrera, and P. Miskovsky, "Modeling, Design and Characterization of a Very Wideband Slot Antenna with Reconfigurable Band Rejection," *IEEE Trans.Antennas Propagat.*, vol.58, no.7, pp. 2218-2225, July 2010.

[21] V.A. Shameena, M.N. Suma, K. Raj Rohith, P.C. Bybi, and P. Mohanan, "Compact ultra-wideband serrated antenna with notch band ON/OFF control," *Electron Lett.,* vol. 42, no.23, pp.1323-1324, 2006

[22] B. Rahmati and H.R. Hassani, "Wideband planar plate monopole antenna with dual tunable notch", *Electron Lett*, vol. 46, pp. 480–481, 2010

[23] Z.H. Hu, P.S. Hall, J.R. Kelly, and P. Gardner, "UWB pyramidal monopole antenna with wide tunable band-notched behaviour", *Electron Lett,* vol.46, pp. 1588–1590, 2011

[24] I.T.E. Elfergani, R.A Abd-Alhameed, C.H. See, S.M.R. Jones and P.S. Excell "A Compact Design of Tunable Band-Notched Ultra-Wide Band Antenna," *Microwave and Optical Technology Letters*, Vol. 54, No. 7, pp. 1642-1644. July 2012.

[25] M. R. Hamid, P. Gardner, P. S. Hall, and F. Ghanem, "Vivaldi With Tunable Narrow Band Rejection," *Microw. Opt. Technol. Lett*., Vol. 53, No. 5, pp.1225-1228, May 2011.

[26] Won-Seok Jeong, Sang-Yun Lee, Won-Gyu Lim, Ho Lim, Jong-Won Yu, "Tunable Band-notched Ultra Wideband (UWB) Planar Monopole Antennas Using Varactor," *In proceeding of Microwave Conference*, *2008, EuMC 2008, 38th European*, pp.266-268, 2008

[27] E. Antonino-Daviu, M. Cabedo-Fabres, M. Ferrando-Bataller and A.Vila-Jimenez, "Active UWB antenna with tunable band-notched behaviour," *Electronics Letters,* vol. 43, no. 18, pp. 959-960, Aug. 2007.

International Journal of RF and Microwave Computer-Aided Engineering, vol. 25, no. 5, pp. 403-412, June 2015, Article first published online: 6 NOV 2014, Wiley Online Library, DOI: 10.1002/mmce.20874; Online ISSN: 1099-047X.

[28] HFSS version 14, Ansys Inc, USA, 2013, Available at: http:// www.ansys.com/

[29] SEMCAD version 14.8, Schmid & Partner Engineering AG, Switzerland Available at: *http://www.speag.com/products/semcad/*

[30] Schantz, H. G., "Radiation efficiency of UWB antennas," *IEEE Conference on Ultra Wideband Systems and Technologies*, pp.351-355, May 2002.

[31] E. H. Newman, P. Bohley, and C. H. Walter, "Two methods for the measurement of antenna efficiency," *IEEE Trans. Antennas Propag.,* vol. 23, pp. 457–461, 1975.

Table and Figures Captions:

Table I: Comparison of the performance of the published tunable and fixed notch wide band antennas. Where λ_O is the wavelength of the lowest operating frequency

Figure 1: (a) Basic antenna structure, (b) Simulated VSWR of the crescent and chorded crescent-shaped proposed antenna with and without defected ground plane

Figure 2: Simulated VSWR with the inner and outer chorded crescent shapes

Figure 3: Input Impedance of the proposed antenna.

Figure 4: The antenna prototype with DC bias circuit, (a) top view (b) bottom view

Figure 5: Cable effect on the antenna performance

Figure 6: Measured and simulated VSWR for proposed loaded varactor antenna with 5 and 11 DC voltages.

Figure 7: Current surface for, (a) the unloaded antenna (b) 0.5 pf loaded antenna, (c) 10.5 pf loaded antenna at 2.4GHz and 3.5GHz.

Figure 8: Simulated against measured normalized antenna radiation patterns for two planes (left: x-z plane, right: y-z plane) at (a) 1.6 GHz, (b) 3.2 GHz and (c) 5.0 GHz.
‘‘ooooo’ simulated co-polarization
‘+++++’ simulated cross-polarization

International Journal of RF and Microwave Computer-Aided Engineering, vol. 25, no. 5, pp. 403-412, June 2015, Article first published online: 6 NOV 2014, Wiley Online Library, DOI: 10.1002/mmce.20874; Online ISSN: 1099-047X.

'——— ' measured co-polarization
'--------' measured cross-polarization

Figure 9: Measured peak gain and radiation efficiency for proposed unloaded and loaded antenna

Table I

Ref	Operating Frequency Band (GHz)	BW (%)	antenna size	Tunability	Tunable notched frequency range (GHz)
13	2.3- 5.8	86.41	0.23 λ_O x 0.30 λ_O x 0.012 λ_O	No	2.96 - 3.17 and 4.13 - 4.95
14	2.0- 5.7	96.10	0.50 λ_O x 0.50 λ_O x 0.18 λ_O	No	2.9–3.0 and 4.6–4.8
15	2.0- 5.7	96.10	0.50 λ_O x 0.50 λ_O x 0.18 λ_O	No	3.39–3.83
16	1.5 – 5.5	114.28	0.28 λ_O x 0.18 λ_O x 0.004 λ_O	No	3.4–3.69
17	3.1–10.6	107.88	0.24 λ_O x 0.37 λ_O x 0.015 λ_O	No	5.15–5.825
18	3.1–10.6	107.88	0.37 λ_O x 0.41 λ_O x 0.010 λ_O	No	5.1–6.2
19	3.1–10.6	107.88	0.37 λ_O x 0.19 λ_O x 0.016 λ_O	No	5.1 to 5.9
20	1.5-5.0	107.69	0.22 λ_O x 0.22 λ_O x 0.007 λ_O	Yes	1.6-2.5
22	3.1– 16.0	56.35	0.41 λ_O x 0.41 λ_O x 0.22 λ_O	Yes	3.9 -4.1 and 5.0-5.5
23	3.1 – 10.0	107.45	0.82 λ_O x 0.82 λ_O x 0.20 λ_O	Yes	4.8 – 7.4
24	3.1 – 10.0	107.45	0.15 λ_O x 0.31 λ_O x 0.05 λ_O	Yes	3.2 – 6.0
25	2.0 – 7.0	111.11	0.46 λ_O x 0.48 λ_O x 0.005 λ_O	Yes	2.0 – 6
26	3.1 – 10.6	107.88	0.72 λ_O x 0.88 λ_O x 0.005 λ_O	Yes	5.2 – 5.8
27	3.1 – 10.6	107.88	1 λ_O x 1 λ_O x 0.19 λ_O	Yes	4.6 – 6.2
Proposed	1.5- 5.5	114.28	0.28 λ_O x 0.18 λ_O x 0.004 λ_O	Yes	2.38 to 3.87

International Journal of RF and Microwave Computer-Aided Engineering, vol. 25, no. 5, pp. 403-412, June 2015, Article first published online: 6 NOV 2014, Wiley Online Library, DOI: 10.1002/mmce.20874; Online ISSN: 1099-047X.

International Journal of RF and Microwave Computer-Aided Engineering, vol. 25, no. 5, pp. 403-412, June 2015, Article first published online: 6 NOV 2014, Wiley Online Library, DOI: 10.1002/mmce.20874; Online ISSN: 1099-047X.

Figure 1:

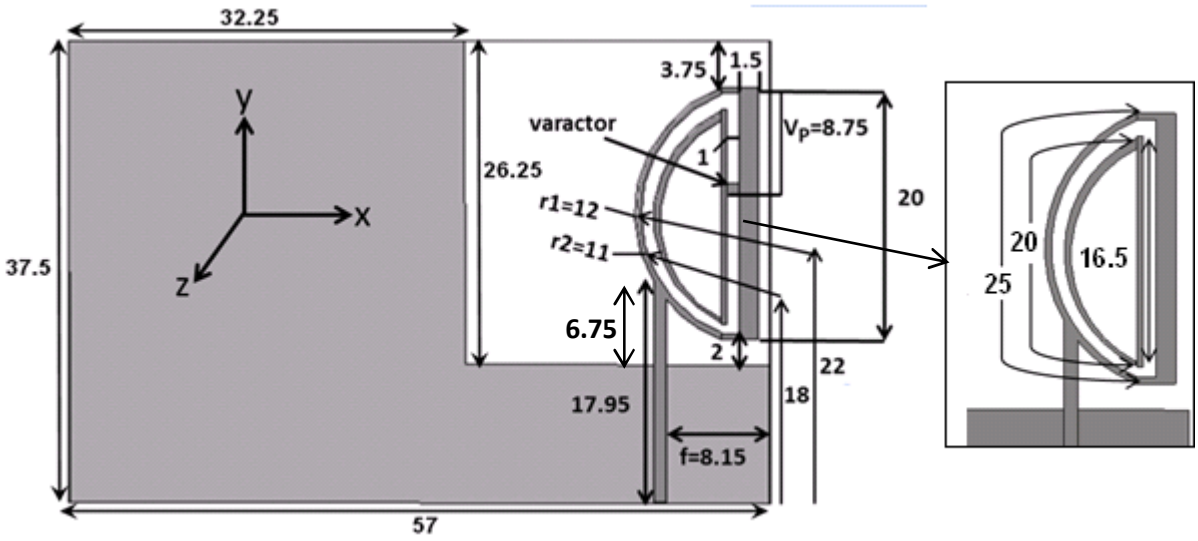

a

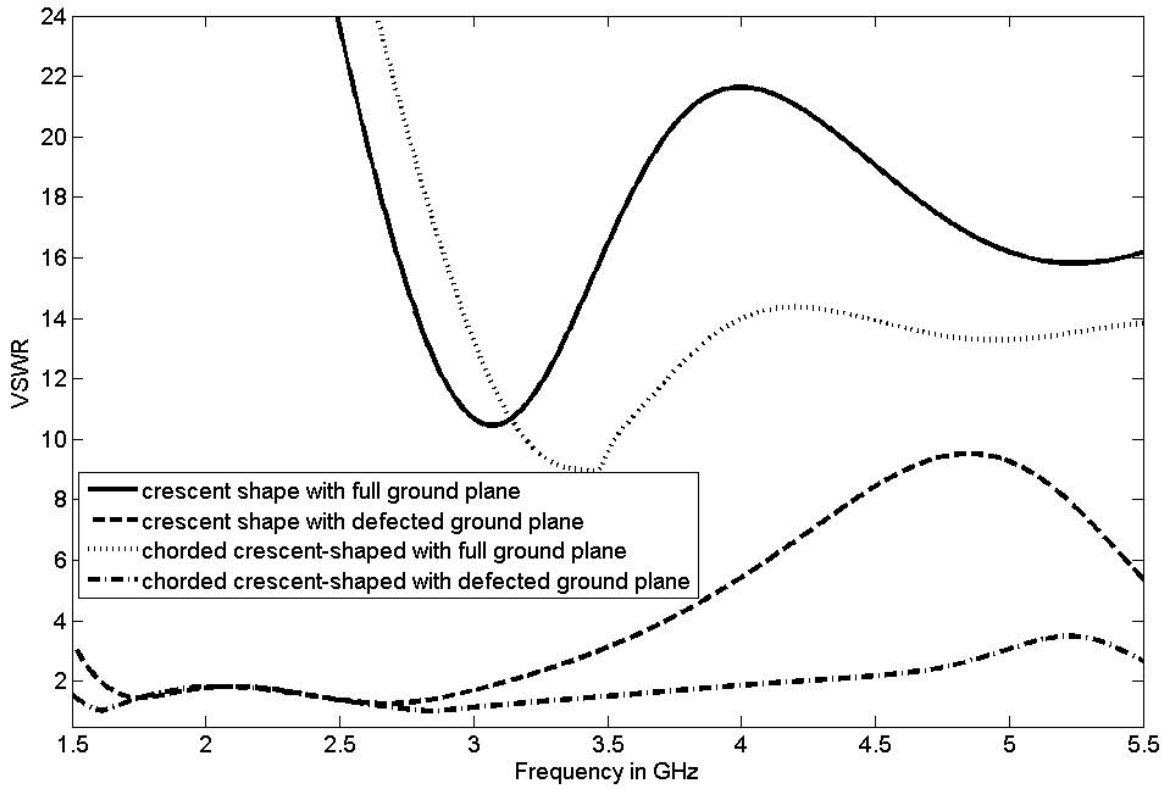

b

International Journal of RF and Microwave Computer-Aided Engineering, vol. 25, no. 5, pp. 403-412, June 2015, Article first published online: 6 NOV 2014, Wiley Online Library, DOI: 10.1002/mmce.20874; Online ISSN: 1099-047X.

Figure 2

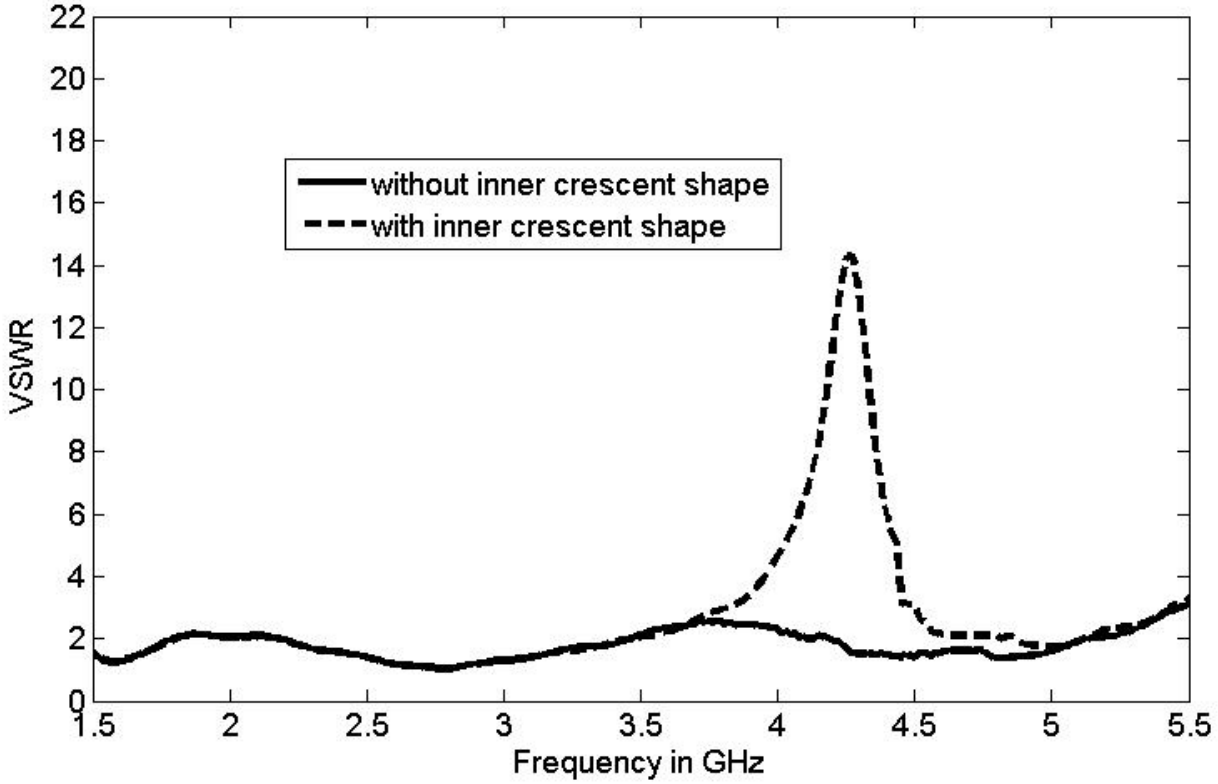

International Journal of RF and Microwave Computer-Aided Engineering, vol. 25, no. 5, pp. 403-412, June 2015, Article first published online: 6 NOV 2014, Wiley Online Library, DOI: 10.1002/mmce.20874; Online ISSN: 1099-047X.

Figure 3:

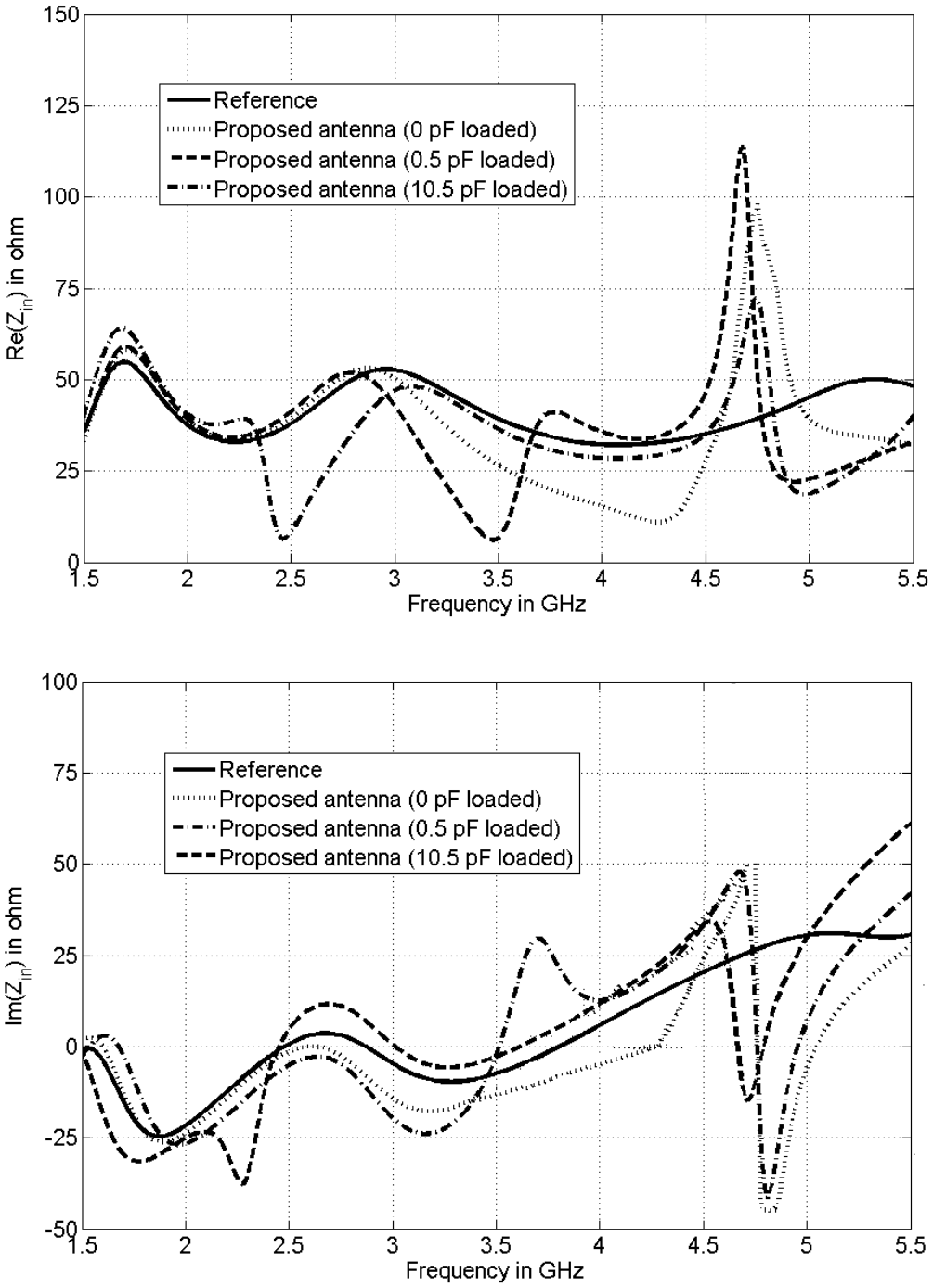

International Journal of RF and Microwave Computer-Aided Engineering, vol. 25, no. 5, pp. 403-412, June 2015, Article first published online: 6 NOV 2014, Wiley Online Library, DOI: 10.1002/mmce.20874; Online ISSN: 1099-047X.

Figure 4:

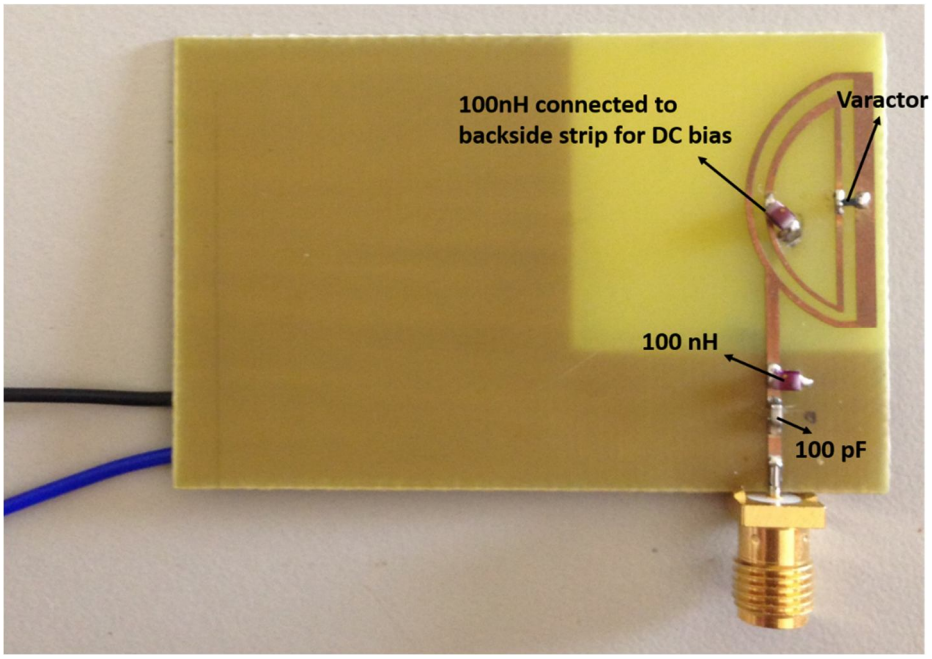

a

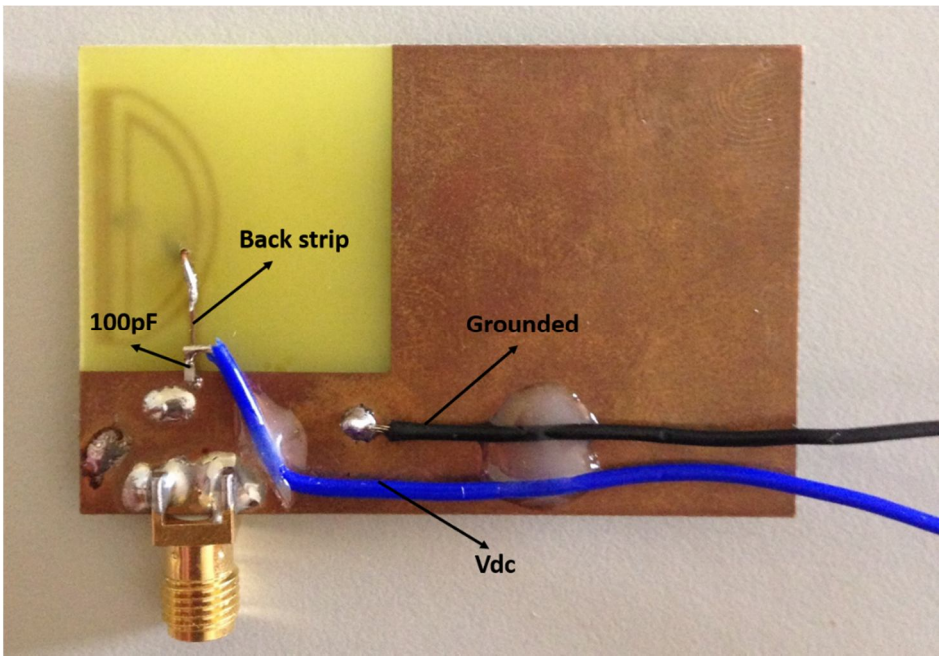

b

International Journal of RF and Microwave Computer-Aided Engineering, vol. 25, no. 5, pp. 403-412, June 2015, Article first published online: 6 NOV 2014, Wiley Online Library, DOI: 10.1002/mmce.20874; Online ISSN: 1099-047X.

Figure 5:

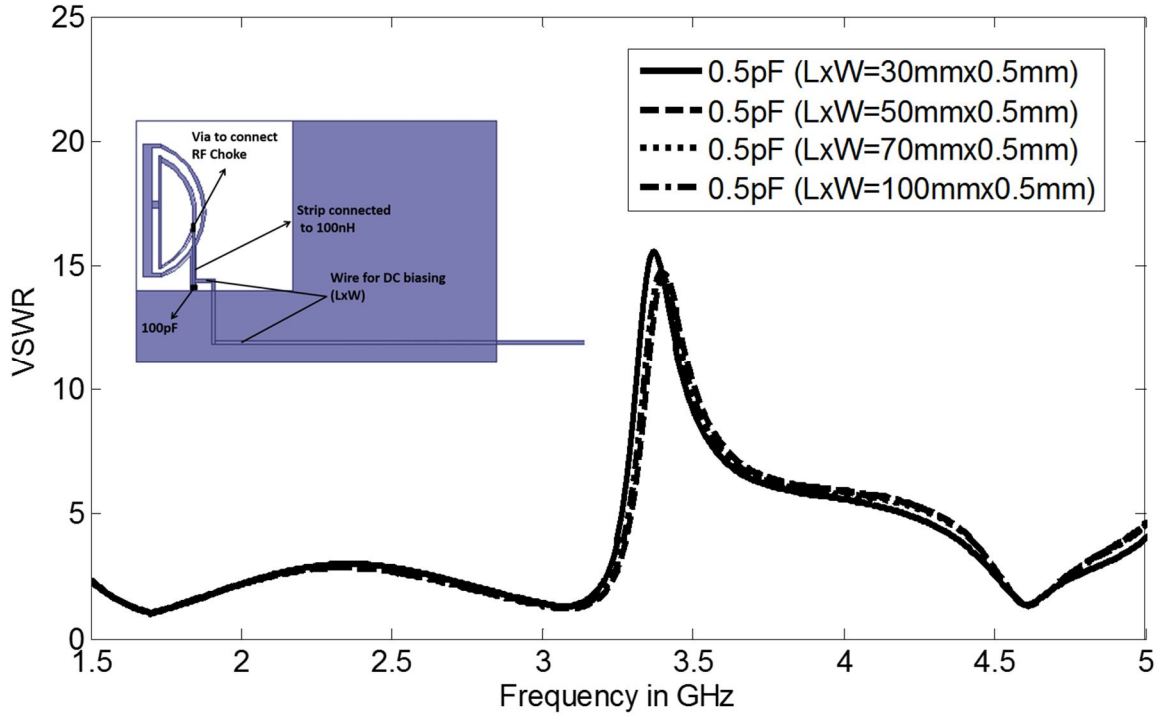

Figure 6:

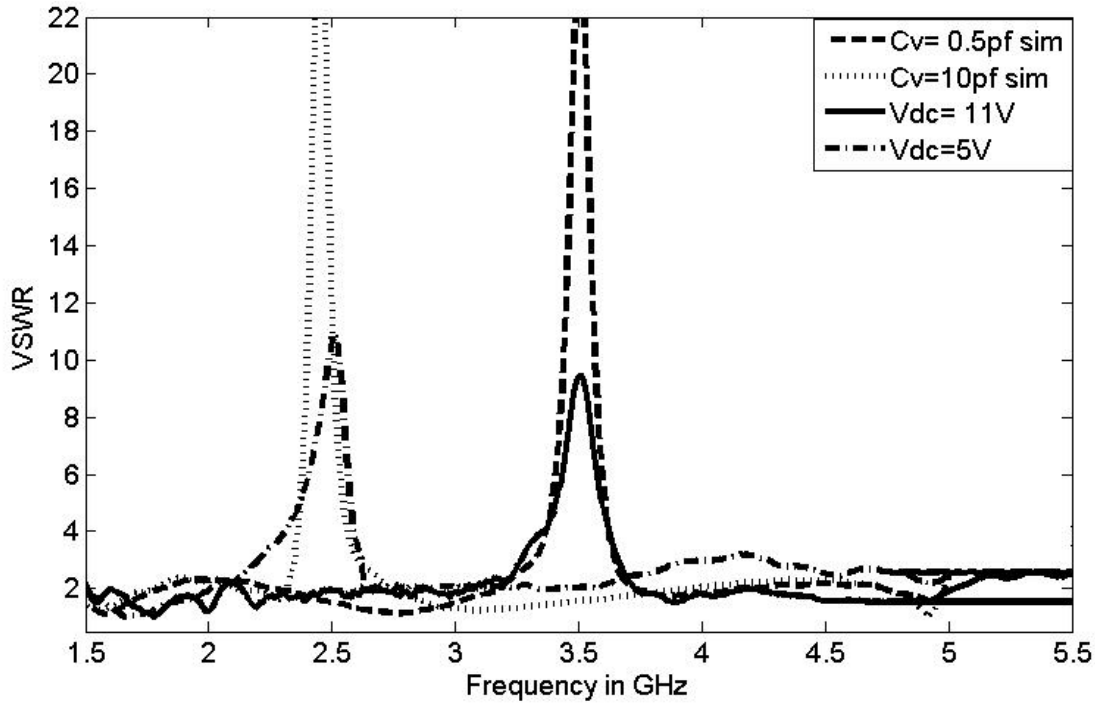

International Journal of RF and Microwave Computer-Aided Engineering, vol. 25, no. 5, pp. 403-412, June 2015, Article first published online: 6 NOV 2014, Wiley Online Library, DOI: 10.1002/mmce.20874; Online ISSN: 1099-047X.

Figure 7:

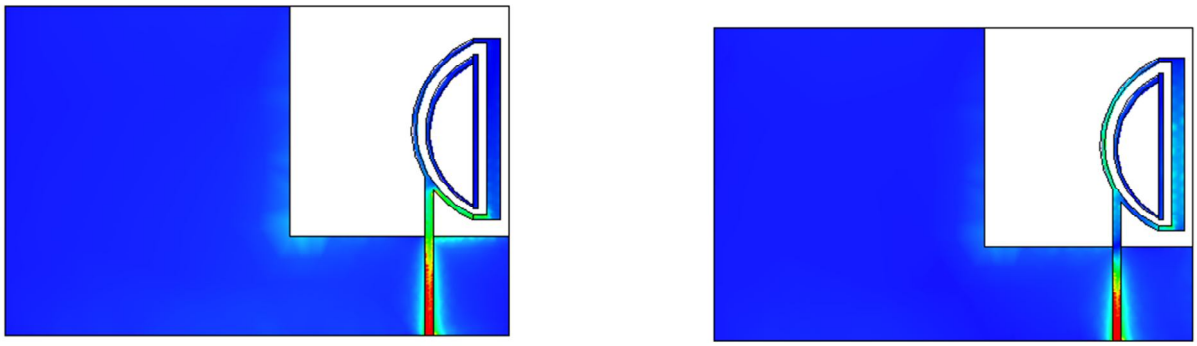

2.4GHz 3.5GHz

a

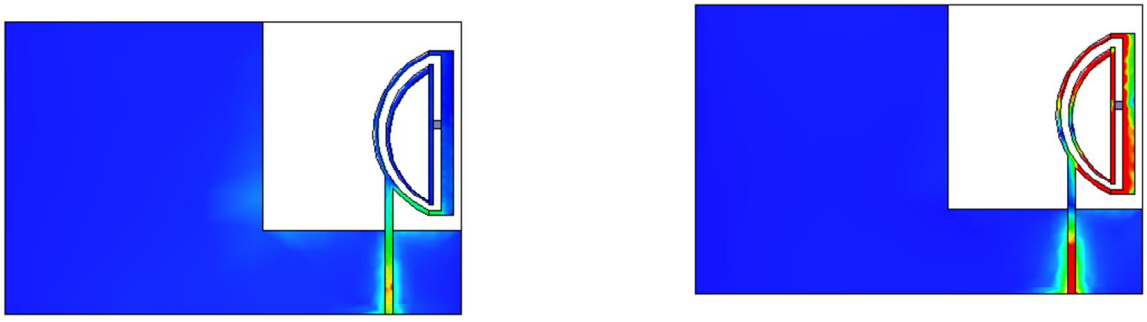

0.5pF at 2.4GHz 0.5pF at 3.5GHz

b

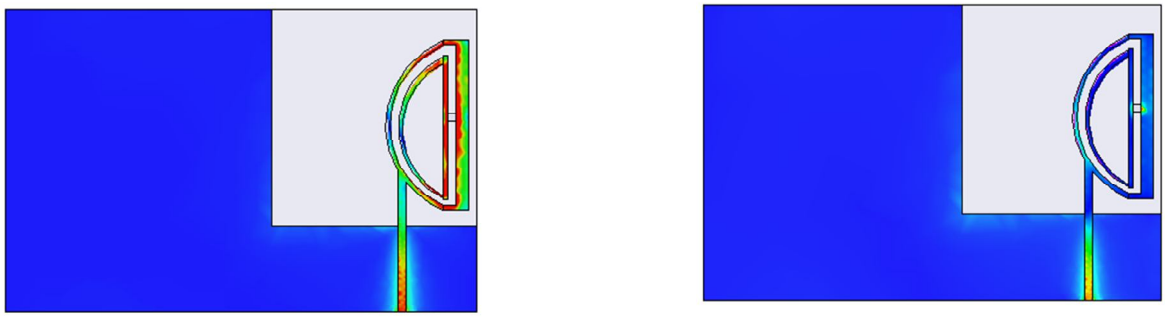

10.5pF at 2.4GHz 10.5pF at 3.5GHz

c

International Journal of RF and Microwave Computer-Aided Engineering, vol. 25, no. 5, pp. 403-412, June 2015, Article first published online: 6 NOV 2014, Wiley Online Library, DOI: 10.1002/mmce.20874; Online ISSN: 1099-047X.

Figure 8:

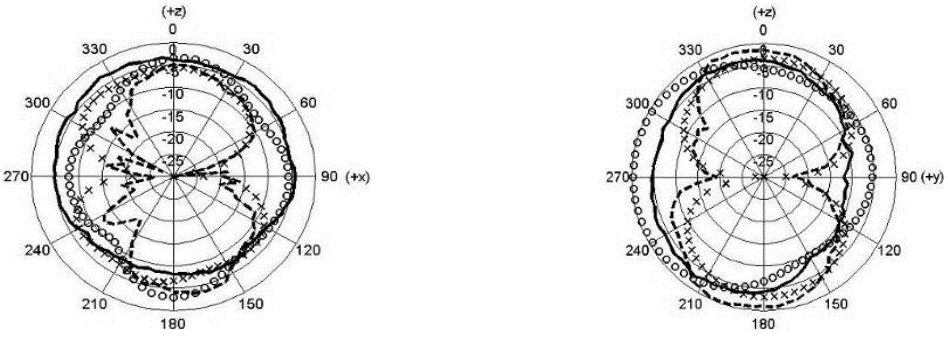

1.6 GHz

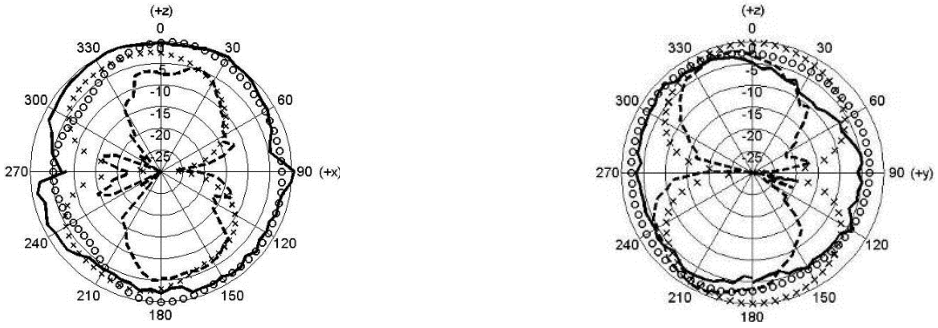

3.2 GHz

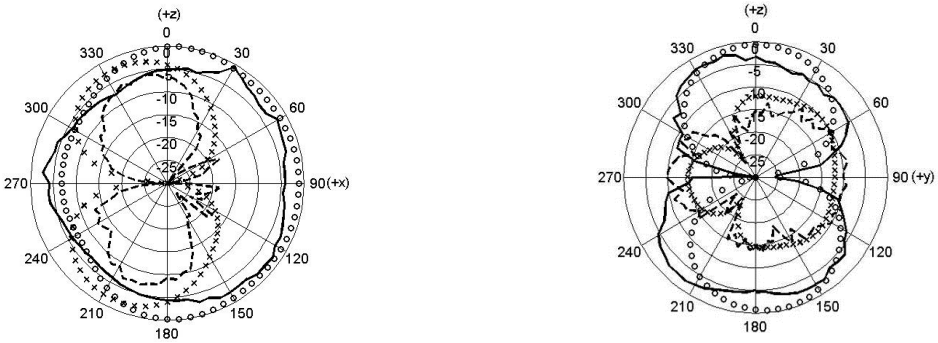

5.0 GHz

International Journal of RF and Microwave Computer-Aided Engineering, vol. 25, no. 5, pp. 403-412, June 2015, Article first published online: 6 NOV 2014, Wiley Online Library, DOI: 10.1002/mmce.20874; Online ISSN: 1099-047X.

Figure 9: